Deformation Behavior and Processing Parameters of Cu-3Ag-0.6Zr Alloy during Compression at Elevated Temperatures

Zhiyong XUE[1,a*], Lingyun GU[1, b], Yu REN[1, c], Xiaoyang HAO[1, d] and Ping XU[1, e]
[1]School of energy, power and mechanical engineering, North China Electric Power University, Beijing 102206, PR China
[a]xuezy@ncepu.edu.cn, [b]cloudgly@126.com, [c]renyu@ncepu.edu.cn,
[d]13269501803@163.com, [e]453544515@qq.com

Abstract. Hot compression tests of the Cu–3Ag–0.6Zr (wt.%) alloy were carried out on a Gleeble-3800 testing machine at various strain rates and at different deformation temperatures. The stress–strain behavior of the alloy during the deformation process are analyzed. The results show that the hot deformation behavior of the Cu–3Ag–0.6Zr alloy is markedly affected by the interaction between the work hardening and the dynamic recrystallization at different strain rates and temperatures. The thermal deformation activation energy is calculated as 248.8384 kJ mol^{-1} and the hot compression constitutive equation has been established. The processing map of the alloy has also been established. According to the obtained processing map, the preferable domains for hot working are identified at a strain rate of 10^{-3} s^{-1} and at 900–940 K or temperatures higher than 1023 K.

1. Introduction

Recently, copper alloys have been considered for aerospace application such as the thrust chamber of liquid rocket engine because of their high thermal conductivity [1]. Although pure copper also has excellent thermal conductivity and is compatible with propellants, the low strength restricts its application in the thrust chamber. Consequently, a small amount of alloying elements (like Ag and Zr) are added to the pure copper to improve its mechanical properties [2]. NARloy-Z alloy is one such alloy designed to manufacture the combustion chamber liner of liquid rocket engine [3, 4].

The plastic deformation performance of metals and alloys under high temperature conditions, which has a significant influence on the hot workability, can be expressed by the relationship between flow stress, strain rate and deformation temperature [5, 6]. However, the hot deformation behavior and processing map of Cu–Ag–Zr alloys has not yet been extensively studied, which is a prerequisite for its usage in hot working processes.

In this paper, compression tests on one particular Cu–Ag–Zr alloy, Cu–3Ag–0.6Zr, were carried out at various strain rates and at different deformation temperatures to reveal its hot

* Corresponding author:xuezy@ncepu.edu.cn

deformation behavior. The stress-strain curves of this alloy were investigated, and the constitutive equation and processing map were established using the experimental data.

2. Material and Experimental Procedure

The Cu–3Ag–0.6Zr (wt.%) alloy investigated was prepared by induction melting. Then the ingot was forged at the temperature range of 1073–923 K. A block with dimensions of 100 mm × 100 mm × 40 mm was cut from the forged piece, and then homogenized at 1193 K for 40 min and water quenched. The cylindrical specimens with 8 mm diameter and 12 mm height were machined from the heat-treated block. Hot deformation experiments were carried out on a Gleeble-3800 testing machine at imposed strain rates of 10^{-3} s^{-1}, 10^{-2} s^{-1}, 10^{-1} s^{-1}, 1 s^{-1} and at testing temperature of 873 K, 923 K, 973 K, 1023 K, respectively, up to a total deformation of 50% (i.e., the true strain is about 0.693). The sample was resistance heated to deformation temperature by thermocoupled-feedback-controlled AC current at a heating rate of 10 K/s and held for 180 s before compression.

3. Results and Discussion

Stress-strain Curves of Cu–3Ag–0.6Zr Alloy. Figure 1 shows the typical true stress-strain curves of the Cu–3Ag–0.6Zr alloy compressed at various strain rates and at different deformation temperatures. At the lowest strain rate (10^{-3} s^{-1}) and the two lower temperatures, the flow stress increases to a maximum value at first and then decreases to a steady state (Fig. 1(a)). Such flow behavior is attributed to the interaction between the work hardening and the dynamic recrystallization (DRX) [6]. In the early stage of hot compression, the work hardening dominates the deformation process and the flow stress increases. Then the work hardening and the softening caused by DRX balance at the point of peak flow stress. As the deformation proceeds, the effect of DRX softening is gradually rising, so the flow stress decreases. DRX softening occurs much earlier as temperature increases to 973 K and 1023 K. When the strain rate rises to 10^{-2} s^{-1} (Fig. 1(b)), the flow stress slowly increases with increasing strain at a relatively low temperature (873 K). As the strain rate further increases to 10^{-1} s^{-1} and 1 s^{-1}, the flow stress of this alloy rises markedly with increasing strain at a temperature lower than 1023 K, as shown in Fig. 1(c) and (d). This suggests that the work hardening plays the dominant role during the entire deformation process. However, the flow stress remains on a steady value as the deformation temperature increases, indicating the balance between the work hardening and dynamic recovery. The flow stress of Cu–3Ag–0.6Zr alloy increases with an increase in strain rate when deformed at the same temperature. However, the thermal softening effect will be more pronounced as the deformation temperature rises.

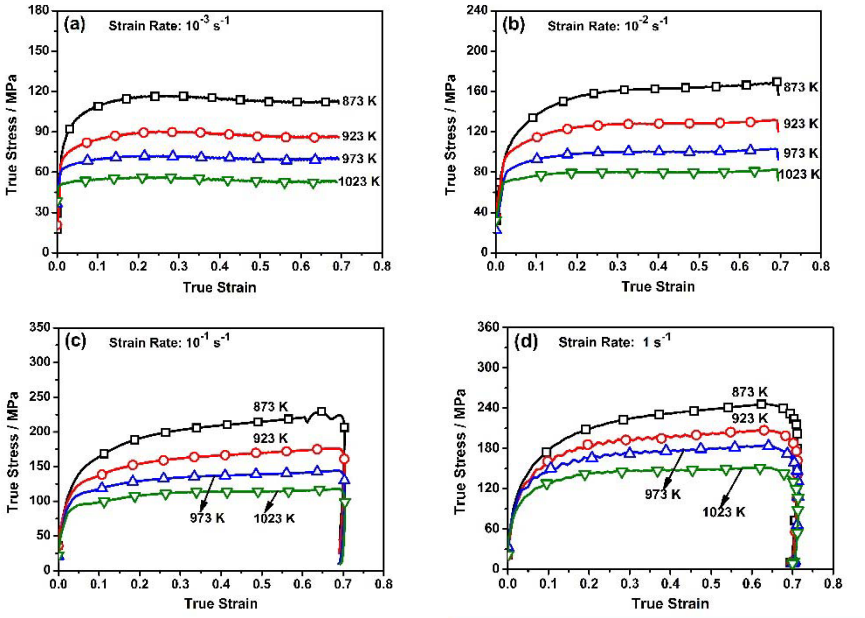

Fig. 1. Typical true stress-strain curves of the Cu–3Ag–0.6Zr alloy compressed at different temperatures with the strain rate of: (a) 10^{-3} s^{-1}, (b) 10^{-2} s^{-1}, (c) 10^{-1} s^{-1}, (d) 1 s^{-1}.

Constitutive Equation. In the hot deformation process of metals, the relationship between strain rate ($\dot{\varepsilon}$), temperature (T) and flow stress (σ) can be expressed as [7]:

$$\dot{\varepsilon} = A \cdot \left[\sinh \left(\alpha \cdot \sigma \right) \right]^{n} \cdot \exp \left(-Q / \left(R T \right) \right) \tag{1}$$

where, A is the structural factor, α is the stress multiplier, n and R are constants, Q is the activation energy. The coefficient Q can be used to characterize the hot workability of materials, which is an important thermodynamic parameter. The power law, Eq. 1, can be expressed as follow if $\alpha \cdot \sigma < 0.8$:

$$\dot{\varepsilon} = A_1 \cdot \sigma^{n_1} \cdot \exp \left(-Q / \left(R T \right) \right) \tag{2}$$

and if $\alpha \cdot \sigma > 1.2$:

$$\dot{\varepsilon} = A_2 \cdot \exp \left(\beta \cdot \sigma \right) \cdot \exp \left(-Q / \left(R T \right) \right) \tag{3}$$

where, β is also a constant, and $\alpha = \beta / n \approx \beta / n_1$ [7].

Taking the natural logarithm on both sides of Eqs. 1, 2 and 3, they are transformed to:

$$\ln \dot{\varepsilon} = \ln A + n \ln \left[\sinh \left(\alpha \sigma \right) \right] - Q / (R T) \tag{4}$$

$$\ln \dot{\varepsilon} = \ln A_1 + n_1 \ln \sigma - Q / (RT) \tag{5}$$

$$\ln \dot{\varepsilon} = \ln A_2 + \beta \cdot \sigma - Q / (RT) \tag{6}$$

In order to calculate α, $\ln \dot{\varepsilon}$ is plotted versus $\ln \sigma$ as shown in Fig. 2(a), and $\ln \dot{\varepsilon}$ is plotted versus σ as shown in Fig. 2(b). From the above, n_1 and β are 7.90543 and 0.06372, respectively, and the value of α is calculated as 0.00806 MPa^{-1} from these values.

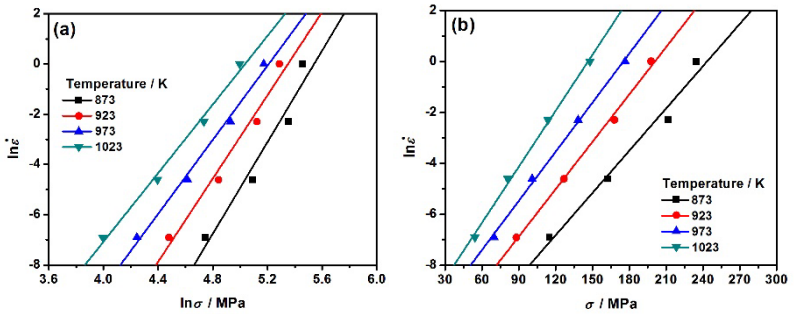

Fig. 2. Relationship between the flow stress and the strain rate: (a) $\ln \dot{\varepsilon} - \ln \sigma$ and (b) $\ln \dot{\varepsilon} - \sigma$.

According to the above natural logarithmic equations, the relationship between the activation energy (Q) and the deformation temperature (T) can be expressed by the following equation:

$$Q = R \cdot \left\{ \frac{\partial \ln [\sinh(\alpha\sigma)]}{\partial (1/T)} \right\}_{\dot{\varepsilon}} \cdot \left\{ \frac{\partial \ln \dot{\varepsilon}}{\partial \ln [\sinh(\alpha\sigma)]} \right\}_{T} \tag{7}$$

The quantity $\ln[\sinh(\alpha\sigma)]$ is plotted versus $1000/T$ in Fig 3(a) and $\ln[\sinh(\alpha\sigma)]$ is plotted versus $\ln \dot{\varepsilon}$ in Fig. 3(b). From the slope of these curves, the value of Q is calculated as 248.8384 kJ mol^{-1}.

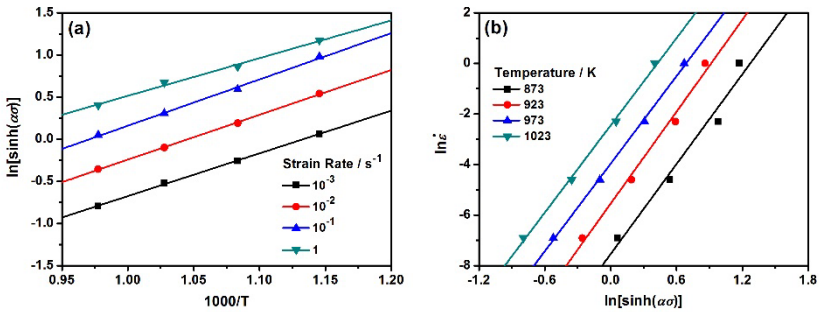

Fig. 3. (a) $\ln[\sinh(\alpha\sigma)] - 1000/T$ and (b) $\ln[\sinh(\alpha\sigma)] - \ln \dot{\varepsilon}$ curves of the Cu–3Ag–0.6Zr alloy.

The relationship between strain rate, deformation temperature and flow stress can also be analyzed using the Zener-Hollomon parameter (*Z*), which is proposed by Sellars and McTegart [8]:

$$Z = A \cdot \left[\sinh \left(\alpha \cdot \sigma \right) \right]^{n} = \exp \left(Q / (\mathrm{R}\,\mathrm{T}) \right) \cdot \dot{\varepsilon} \tag{8}$$

Taking the natural logarithm on both sides, Eq. 8 is transformed to:

$$\ln Z = \ln A + n \cdot \ln \left[\sinh \left(\alpha \cdot \sigma \right) \right] = Q / (\mathrm{R}\,\mathrm{T}) + \ln \dot{\varepsilon} \tag{9}$$

In order to calculate *n* and $\ln A$, $\ln Z$ is plotted versus ln[sinh($\alpha\sigma$)] as shown in Fig. 4. The slope *n* is calculated as 5.87049 and the intercept $\ln A$ as 26.83336, so *A* is 4.50381×10^{11} s^{-1}.

Based on above analysis, the constitutive equation of the Cu–3Ag–0.6Zr alloy is determined as:

$$\dot{\varepsilon} = 4.50381\times10^{11} \cdot \left[\sinh \left(0.00806 \cdot \sigma \right) \right]^{5.87049} \cdot \exp \left(-\frac{248838.4}{8.31447 \cdot T} \right) \tag{10}$$

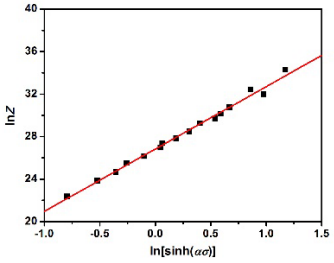

Fig. 4. Relationship between $\ln Z$ and ln[sinh($\alpha\sigma$)] of the Cu–3Ag–0.6Zr alloy.

Processing Map. The processing map for the Cu–3Ag–0.6Zr alloy obtained at a true strain of 0.55 is shown in Fig. 5, which is constructed by overlapping a power dissipation map and an instability map. In fact, processing maps made at different strains are essentially similar [9]. The processing map is classified into two regions: stability domain (unshaded) and instability domain (shaded). The contour lines represent the efficiency of power dissipation, which corresponds to the microstructural changes during hot deformation [6]. Figure 5 shows that the alloy is not suitable for processing under high strain rates. The efficiency of power dissipation increases with decreasing strain rate. However, as the deformation temperature increases, the stability domain gradually expands, implying the reduction in the possibility of unstable deformation of the Cu–3Ag–0.6Zr alloy. The suitable hot processing temperature is about 900–940 K or a temperature higher than 1023 K according to this processing map. In both domains the efficiency of power dissipation amounts to 31%.

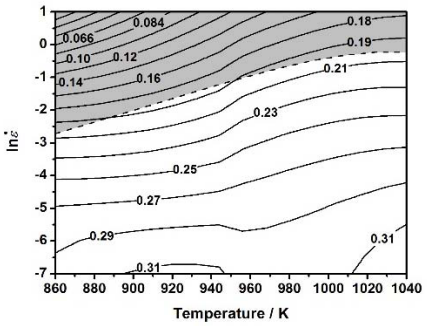

Fig. 5. Processing map obtained at a true strain of 0.55.

4. Conclusions

Hot compression tests of the Cu–3Ag–0.6Zr alloy were carried out on a Gleeble-3800 testing machine at strain rates from 10^{-3} s^{-1} to 1 s^{-1} and deformation temperatures between 873 and 1023 K. The major conclusions are as follows:

(1) The stress–strain behavior of the Cu–3Ag–0.6Zr alloy at various strain rates and at different deformation temperatures can be categorized into two types. At a low strain rate (10^{-3} s^{-1}), the plastic deformation behavior is determined by the interaction between the work hardening and the dynamic recrystallization. At high strain rates (above 10^{-2} s^{-1}), the work hardening plays a main role on the whole deformation process of this alloy. The flow stress decreases with increasing deformation temperature and/or decreasing strain rate.

(2) The relationship between strain rate, temperature and flow stress of the Cu–3Ag–0.6Zr alloy can be expressed by the constitutive equation:

$$\dot{\varepsilon}=4.50381\times10^{11}\cdot\left[\sinh\left(0.00806\cdot\sigma\right)\right]^{5.87049}\cdot\exp\left(-\frac{248838.4}{8.31447\cdot T}\right)$$

(3) The processing map of the Cu–3Ag–0.6Zr alloy has been established. The preferable domains for hot working are identified at a strain rate of 10-3 s-1 and 900–940 K or at a strain rate of 10^{-3} s^{-1} and at temperatures higher than 1023 K. In both domains the efficiency of power dissipation amounts to 31%.

5. Acknowledgment

This study was financed by the Program for New Century Excellent Talents in University (NCET-12-0849) and the Fundamental Research Funds for the Central Universities (2014ZZD03 and 13ZD12).

References

1. S. C. Krishna, K. T. Tharian, B. Pant, R. S. Kottada, Microstructure and mechanical properties of Cu-Ag-Zr alloy, J. Mater. Eng. Perform. 22 (2013) 3884-3889.Gaganov, J. Freudenberger, E. Botcharova, L. Schultz, Effect of Zr additions on the microstructure, and the mechanical and electrical properties of Cu–7 wt.%Ag alloys, Mater. Sci. Eng. A 437 (2006) 313-322.

2. J. H. Sanders, P. S. Chen, S. J. Gentz, R. A. Parr, Microstructural investigation of the effects of oxygen exposure on NARloy-Z, Mater. Sci. Eng. A 203 (1995) 246-255.
3. J. Singh, G. Jerman, R. Poorman, B. N. Bhat, A. K. Kuruvilla, Mechanical properties and microstructural stability of wrought, laser, and electron beam glazed NARloy-Z alloy at elevated temperatures, J. Mater. Sci. 32 (1997) 3891-3903.
4. H. Zhang, H. Zhang, L. Li, Hot deformation behavior of Cu–Fe–P alloys during compression at elevated temperatures, J. Mater. Process. Tech. 209 (2009) 2892-2896.
5. Z. Ding, S. Jia, P. Zhao, M. Deng, K. Song, Hot deformation behavior of Cu–0.6Cr–0.03Zr alloy during compression at elevated temperatures, Mater. Sci. Eng. A 570 (2013) 87-91.
6. H. J. McQueen, N. D. Ryan, Constitutive analysis in hot working, Mater. Sci. Eng. A 322 (2002) 43-63.
7. C. M. Sellars, W. J. Mctegart, On the mechanism of hot deformation, Acta Metall. 14 (1966) l136-1138.Sivakesavam, Y. V. R. K. Prasad, Characteristics of superplasticity domain in the processing map for hot working of as-cast Mg–11.5Li–1.5Al alloy, Mater. Sci. Eng. A 323 (2002) 270-277.